ACS APPLIED MATERIALS & INTERFACES

Research Article

www.acsami.org

Anisotropic Wetting of Microstructured Surfaces as a Function of Surface Chemistry

Sonja Neuhaus,[†,‡] Nicholas D. Spencer,[‡] and Celestino Padeste*[,†]

[†]Laboratory for Micro- and Nanotechnology, Paul Scherrer Institut, 5232 Villigen PSI, Switzerland

[‡]Laboratory for Surface Science and Technology, Department of Materials, ETH Zurich, Wolfgang-Pauli-Strasse 10, 8093 Zurich, Switzerland

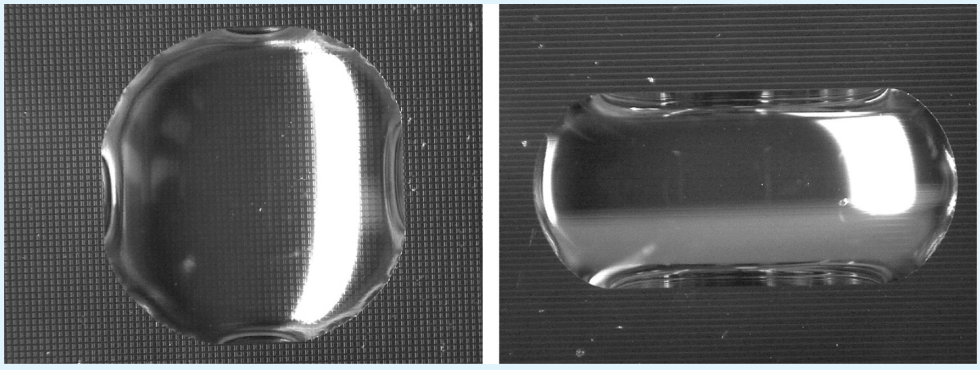

ABSTRACT: In order to study the influence of surface chemistry on the wetting of structured surfaces, microstructures consisting of grooves or squares were produced via hot embossing of poly(ethylene-*alt*-tetrafluoroethylene) ETFE substrates. The structured substrates were modified with polymer brushes, thereby changing their surface functionality and wettability. Water droplets were most strongly pinned to the structure when the surface was moderately hydrophilic, as in the case of poly(4-vinylpyridine) (P4VP) or poly(vinyl(*N*-methyl-2-pyridone) (PVMP) brush-modified substrates. As a result, the droplet shape was determined by the features of the microstructure. The water contact angles (CA) were considerably higher than on flat surfaces and differed, in the most extreme case, by 37° when measured on grooved substrates, parallel and perpendicular to the grooves. On hydrophobic substrates (pristine ETFE), the same effects were observed but were much less pronounced. On very hydrophilic sampes (those modified with poly(*N*-methyl-vinylpyridinium) (QP4VP)), the microstructure had no influence on the drop shape. These findings are explained by significant differences in apparent and real contact angles at the relatively smooth edges of the embossed structures. Finally, the highly anisotropic grooved microstructure was combined with a gradient in polymer brush composition and wettability. In the case of a parallel alignment of the gradient direction to the grooves, the directed spreading of water droplets could be observed.

KEYWORDS: *microstructure, hot embossing, polymer brush, wetting anisotropy, wettability gradient*

INTRODUCTION

Directional wetting is a desirable materials property, particularly in the context of self-cleaning surfaces. Nature provides some very sophisticated strategies for the implementation of directional wetting. Illustrative examples include the surface structures of a rice leaf[1] or of the wing of the morpho aega butterfly.[2,3] Learning from these and other examples, it has been recognized that an anisotropic surface topography can, in general, facilitate cleaning by directing water droplets and by increasing the water contact angle due to the underlying micro- and nanostructure.[4]

A variety of approaches have been adapted in order to study and mimic the properties of anisotropic surfaces, although the methods for pattern creation, the pattern dimensions and the properties studied have varied widely. Xia et al. applied interference lithography in photoresist materials for the creation of submicrometer-scale periodic surfaces exhibiting highly anisotropic wetting. Further treatments with low-pressure plasma and different process gases resulted in a modification of the surface chemistry, and, consequently, in hydrophilic or hydrophobic surfaces. An important finding was that the periodicity and the duty cycle of the structure only had a modest influence on the anisotropy.[5] Groove structures with large periods and very large heights on the order of tens to hundreds of micrometers were prepared by wafer dicing.[6] Subsequent coating with a fluoroalkylsilane resulted in superhydrohobic surfaces on which substantial differences in sliding angles in orthogonal directions were observed. A detailed study of wettability was conducted on a variety of complex surface topographies with translational symmetry on

Received: August 17, 2011
Accepted: December 9, 2011
Published: December 9, 2011

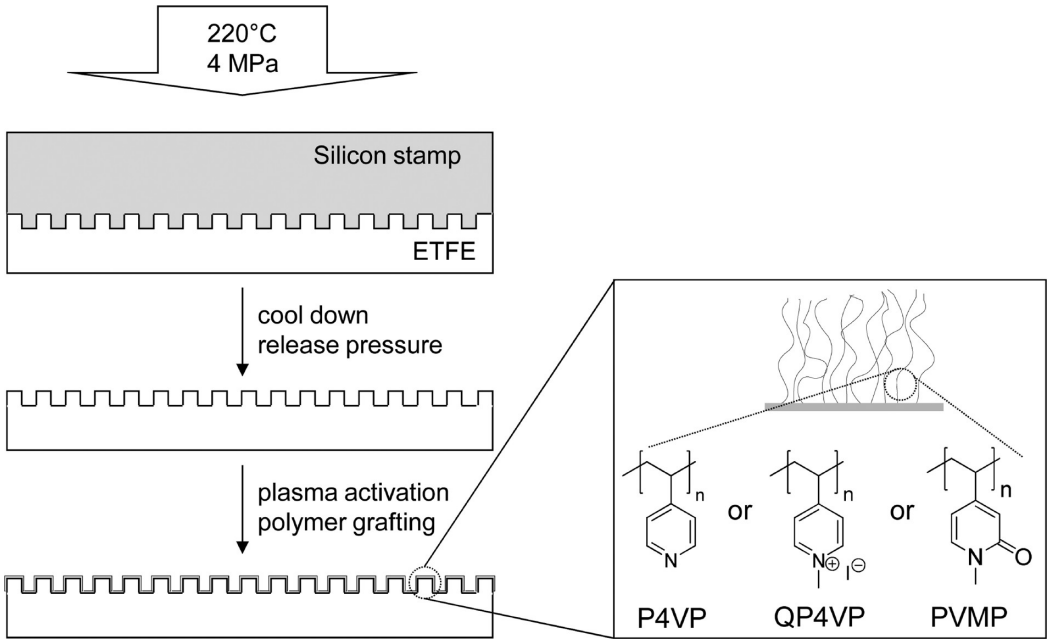

Figure 1. Preparation of microstructured ETFE by hot embossing of a silicon stamp. To functionalize the surface with polymer brushes, we activate the samples with atmospheric-pressure helium plasma, and a graft reaction with 4-vinylpyridine is subsequently carried out. In a further step, P4VP can be transformed to QP4VP by quaternization, and QP4VP can in turn be transformed into PVMP. These brushes are known to show different wetting properties.[14,15]

cast elastomeric poly(dimethylsiloxane) (PDMS) surfaces. The main finding was that the static and dynamic contact angle anisotropy was reduced but not eliminated on surfaces with discontinuous ridges.[7] Microwrinkling of PDMS surfaces by a combination of UV/ozone treatment and application of mechanical strain was exploited to produce surfaces with wrinkles having a tunable amplitude-to-wavelength ratio. Water droplets assumed an elongated, parallel-sided shape on these highly anisotropic substrates. Because of this particular drop shape, strongly differing CAs parallel and perpendicular to the line structure were observed and explained by a pinning of the droplets' contact line along the line features. This pinning results from an energy barrier to the spreading of the droplet perpendicular to the lines. In contrast, the motion of the contact line was not hindered in the direction parallel to the lines.[8] Similarly, drop-shape anisotropy and anisotropies in static and dynamic contact angles were observed on surfaces with lines (1−20 μm) consisting of hydrophobic silanes.[9] In a study dealing with the influence of the water-drop volume on the observed wetting anisotropy, the microstructured substrates were prepared by hot embossing of poly(methacrylic acid) (PMMA) sheets and subsequent deposition of plasma-polymerized polymers to alter the wettability of the surface. The use of droplet volumes ranging from picoliters to microliters resulted in a significant variation in contact angles, and the importance of reporting the droplet volume along with the CA when using very small droplets was emphasized.[10]

Surfaces with anisotropic properties can potentially be used to induce the directed and, more importantly, spontaneous movement of water. For instance, it has been demonstrated that a roughness gradient on silicon surfaces modified with a fluorosilane led to the movement of a 10 μL sized droplet.[11] Another potent driving force is a gradient in surface free energy as demonstrated by Chaudhury and Whitesides.[12] In this case, a wettability gradient was created by varying the surface coverage of a hydrophobic self-assembled monolayer (SAM). The resulting difference in surface free energy was large enough to make "water run uphill", i.e., against an inclination of 15°. Yet again, the most sophisticated concepts can be found in nature, e.g., in the directional water collection on wetted spider silk. The structural features of these complex fibers give rise to local surface energy gradients and differences in Laplace pressure, both factors cooperating to yield the unique properties of this material. Zheng and co-workers have succeeded in preparing an artificial fiber which mimics the wetting properties of spider silk by immersing an uniform nylon fiber in a solution of PMMA in *N*,*N*-dimethylformamide and ethanol. Quick withdrawal in a horizontal manner resulted in a thin liquid polymer film on the fiber surface that subsequently broke up into tiny solution drops. After drying, features similar to the spindle knots observed on spider silk were obtained.[13]

In this work, drop shape and contact-angle anisotropy were studied as a function of surface topography and surface functionality. Moreover, contact line pinning, i.e. the retention of the three-phase contact line of the droplet on features of the microstructure, was investigated. A wettability range resulting in very strong anisotropy was identified. Consequently, by creating a wettability gradient in this range, the directed spreading of water droplets could be induced on grooved substrates. In order to produce microstructured samples with tailorable surface chemistry, two established methods, namely hot embossing of polymer foils and grafting of polymer brushes from polymer surfaces were combined (Figure 1). Structured surfaces were produced in thin foils (100 μm) of poly(ethylene-*alt*-tetrafluoroethylene) (ETFE) by hot embossing. Subsequently, the surface was modified by grafting of polymer brushes following cold, atmospheric-pressure plasma activation. In our previous study, it was shown that the wettability of intrinsically hydrophobic ETFE (water contact angle ~101°) could be tailored over a wide range by choosing the appropriate monomer functionality and by performing chemical modifications after the grafting step.[14] Here, brushes of poly(4-

vinylpyridine) (P4VP), a weak polyelectrolye (PEL), were chosen because of their intermediate water contact angle (CA) on flat surfaces (48°). Additionally, the pyridine moieties can be transformed to charged pyridinium groups in a quaternization reaction, yielding a cationic polyelectrolyte brush (QP4VP), which imparts highly hydrophilic properties (CA ~10°) to the surface. The QP4VP brush can, in turn, be transformed into a neutral PVMP brush having a CA between P4VP and the hydrophobic ETFE substrate. Moreover, the time-dependent character of the transformation from QP4VP to PVMP allowed for the preparation of a wettability gradient.[15]

EXPERIMENTAL SECTION

Materials. 4-Vinylpyridine (4VP, 95%, Aldrich, Switzerland), poly(ethylene glycol) (PEG, average M_n 380−420, Aldrich, Switzerland), methyl iodide (MeI, >99%, Fluka, Switzerland), nitromethane (CH_3NO_2, puriss. ≥ 98.5%, over molecular sieve, Sigma-Aldrich, Switzerland), sodium hydroxide (NaOH, p.a., Merck, Switzerland), isopropanol (analytical grade, VWR, Switzerland), ethanol (analytical grade, VWR, Switzerland), and acetone (analytical grade, VWR, Switzerland) were used as received. Water used for rinsing or as a solvent was ultrapure (resistivity 18.2 MΩ cm, Millipore, Billerica, MA, USA).

Methods. *Hot Embossing of ETFE Foils.* ETFE samples with hot-embossed periodic grooves or squares were prepared as follows: Stamps with the desired structures were produced using standard photolithography and reactive-ion etching. 100 μm thick ETFE foils (Nowoflon, ET-6235 Nowofol GmBH, Siegsdorf, Germany) were placed between the stamp and a polished silicon wafer. After heating to 220 °C in a Jenoptik HEX03 press (Jenoptik GmbH, Germany), a pressure of 4 MPa was applied for for 20 min. The system was cooled to room temperature before the pressure was released. The assembly was then removed from the press and separated using a razor blade.

Cold Atmospheric-Pressure-Plasma Treatment. Hot-embossed ETFE samples were cut into pieces with a scalpel. After thorough rinsing with ethanol and acetone, the pieces were dried in a stream of nitrogen and fixed to glass microscope slides with adhesive tape. The samples were then activated with cold, atmospheric-pressure helium plasma by repeatedly passing the nozzle of a piezobrush (PZ1, Reinhausen Plasma GmbH, Regensburg, Germany) at a distance of about 1 cm over the surface for 20−25 s. This nonthermal plasma is of the capacitive discharge type with an rf power supply (135 kHz, 20 W) and an output voltage of 1.8 kV. Helium (6.0) was supplied at a flow rate of 22 L/min. The plasma temperature was lower than 40 °C (manufacturer's information). Plasma-treated samples were allowed to stand in air for 10 min and were then rinsed with ethanol and blown dry with nitrogen prior to grafting.

Grafting of P4VP from Surfaces via Free-Radical Polymerization. A solution of 4VP (50 vol%) in PEG was degassed with argon for 10 min. PEG was added to increase the viscosity of the monomer solution, as this has been found to promote the growth of polymer brushes.[16] Then, the activated samples were rinsed with ethanol, blown dry with nitrogen, and added to the vial, which was sealed with a rubber septum and degassed for another 15 min. The vial was placed in an oil bath and heated to 60 °C for 1 h. The samples were washed and immersed in ethanol and then treated in an ultrasonic bath for 10 min.

Quaternization of P4VP. The samples were rinsed with water and then immersed in a solution of methyl iodide (0.3 mL, 5 mmol) in nitromethane (3 mL). The solution was degassed for 15 min and then heated to 45 °C for 8 h. After the reaction, the samples were rinsed with nitromethane, immersed in isopropanol, and treated in an ultrasonic bath for 10 min, and then rinsed with water.

Transformation of QP4VP to PVMP. Samples modified with quaternized QP4VP were immersed for 40′ in 0.1 M NaOH to transform the strong polyelectrolyte brush into a neutral PVMP brush. The samples were then thoroughly rinsed with water.

Preparation of QP4VP/PVMP Gradient Samples. Gradient samples were prepared as described previously by slowly immersing samples modified with QP4VP brushes into a 0.1 M NaOH solution at room temperature.[15] For this purpose, a programmable 3-axis robot of the "Industry Roboter" series from FischerTechnik (Waldachtal, Germany) was used. The parameters were chosen such that the sample was moved downward at about 1 mm/min for 20 min. After this time, the sample was thoroughly rinsed with water and blown dry with nitrogen.

Scanning Electron Microscopy (SEM). Samples were sputter-coated with a thin chromium layer and imaged on a Zeiss Supra VP55 high-resolution, field-emission scanning electron microscope (Carl Zeiss, Germany).

Atomic Force Microscopy (AFM). Measurements were performed in TappingMode in air on a Dimension IIIa instrument (Veeco, Germany) using silicon cantilevers (NSC15/AlBS, Mikromasch, CA, USA) with a Si_3N_4 coating and a tip radius of 20 nm, a spring constant of 40 N/m and a resonance frequency of 325 kHz (manufacturer's specifications).

Contact-Angle Determination. Water drops of 2 μL volume were placed on the sample with a micropipet (Pipetman P2, Gilson Middleton, WI, USA) and images were recorded with a microscope camera (DigiMicro 2.0, dnt GmbH, Germany). Contact-angle evaluation was performed with the contact-angle PlugIn of the ImageJ software (version 1.38x, National Institutes of Health, US). The error in contact-angle determination is estimated to be ±3°.

Sliding-Angle Determination. The sample was mounted on a glass slide with adhesive tape. The glass slide was then continuously tilted until the drop started moving or the tilt angle was 90°. Sliding angles were determined from images recorded with a microscope camera (DigiMicro 2.0, dnt GmbH, Germany).

Determining Drop Dimensions and Drop Anisotropy. Water droplets (2 μL) were placed on the sample and images in top view were recorded with a digital camera (Nikon Coolpix 4500) mounted on a Leica MZ 95 optical microscope. A piece of millimeter paper was used as a reference for the determination of absolute drop sizes. The drop shape ratio was calculated by dividing the drop dimension along the grooves by the drop dimension perpendicular to the grooves, or in the case of foils embossed with squares by dividing the drop dimensions determined in perpendicular directions.

To obtain images of the droplet footprints, we mounted samples on glass microscope slides. After deposition of a water droplet (0.5 or 2 μL volume), images were recorded from below with a microscope camera. The ratio of straight, pinned droplet sections to the drop circumference were determined by manual evaluation with the ImageJ software.

RESULTS AND DISCUSSION

Preparation of Microstructured ETFE Surfaces and Functionalization with Polymer Brushes. In order to assess the influence of the surface microstructure on the drop shape and water contact angles, surfaces with grooves or with a square pattern were prepared by hot embossing. In the case of the highly anisotropic grooved surfaces, the most pronounced differences in CA are expected along and perpendicular to the grooves, while on square patterns different surface properties are expected along the edge of the squares and along the square diagonal, i.e., at an angle of 45°. In Figure 2, SEM images of the obtained structures are shown. The protruding features of the silicon stamp were faithfully reproduced in the fluoropolymer foil by applying high temperature and pressure for a period of 20 min. However, under the embossing conditions the polymer did not completely fill the rectangular profiles of the structures, leading to rounded edges at the top of the replicated structures. Line profiles measured with AFM allowed the minimal radius of curvature to be estimated at about 700 nm. (As this value is much larger than the radius of the used tip, convolution effects

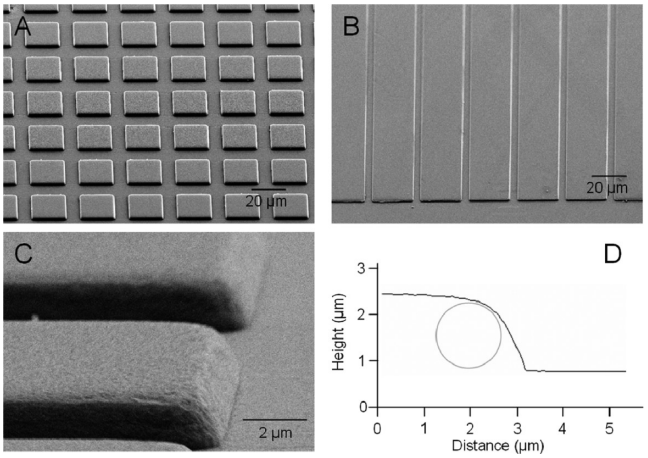

Figure 2. (A–C) SEM images of the embossed groove and square structures. Dimensions: squares 21 μm, gaps 9 μm (period 30 μm), lines 24 μm, grooves 5 μm (period 29 μm). Images were taken at viewing angles of 45° (A and B) and 10° (C). D: AFM line profile measured at the edge of a square structure. The circle indicates the estimated minimum curvature (r = 700 nm) at the top edges of the structures.

are negligible in this estimation). To tailor the wettability of the microstructured surface, we grafted and modified P4VP brushes as described earlier.[14] Briefly, radical initiators were created on the surface of ETFE by activation with cold, atmospheric-pressure helium plasma. In a subsequent free-radical polymerization, polymer brushes were grown. Owing to the strong covalent attachment of the brush and the excellent chemical stability of the substrate, modification of the neutral polymer brush after grafting to yield a charged polyelectrolyte brush, poly(*N*-methyl-vinylpyridinium) (QP4VP), was possible. Moreover, a brush having a wettability in between the moderately hydrophilic P4VP brushes and the hydrophobic ETFE substrate was produced by transforming the strong polyelectrolyte QP4VP to the neutral poly(vinyl(*N*-methyl-2-pyridone) (PVMP) under alkaline conditions, as described elsewhere.[15] The chemical compositions of all surfaces investigated here have been characterized in detail by means of ATR-IR and UV/vis spectroscopy.[14,15] AFM measurements showed that the grafted layer, which is estimated to be below 100 nm in thickness, has no significant influence dimensions of the grafted structures.

In the following, we will use the terms "grooved" and "squared" for the two structures and "neutral", "weak PEL", and "ionic" for the modifications with PVMP, P4VP, and QP4VP, respectively.

Drop Shape and Water-Contact-Angle Anisotropy. Panels A and B in Figure 3A illustrate the influence of the microstructure on the shape of a water droplet as a function of surface chemistry and topography. The top view illustrates that, except for the case where the surface was modified with a very hydrophilic brush (QP4VP), the drop shape was determined by the underlying microstructure. On the square microstructure, the droplet shape deviates strongly from circularity, whereas elongated droplets were observed on grooved surfaces. The effect was most pronounced in the case of surfaces modified with neutral and weak PEL brushes (PVMP and P4VP), where the drop circumferences contained long straight sections along the microstructure axes. Therefore, the drop shape was apparently also strongly influenced by the hydrophilicity of

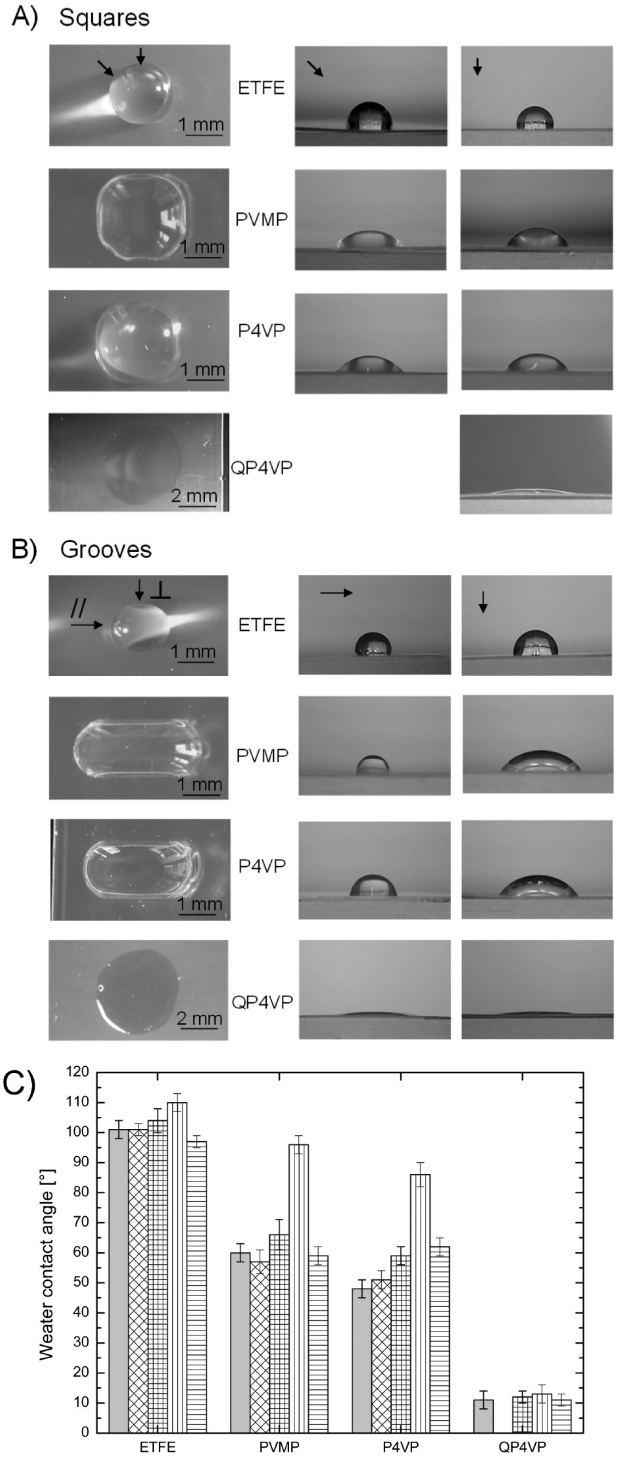

Figure 3. (A) Images of water droplets (2 μL) on samples with a periodic square microstructure with ETFE in the pristine state and after modification with neutral (PVMP), weak PEL (P4VP) or ionic (QP4VP) polymer brushes. Observation from above and from the side along the pattern diagonal and along the square edge direction (indicated with arrows). (B) As in A, but on grooved microstructures. Observation from above and from the side, with viewing directions along and perpendicular to the groove direction. (C) Water CAs on flat (gray bar) and microstructured surfaces. Surfaces with square pattern: observation along the square diagonal (cross-hatched) and along the square edge (hatched). On grooved surfaces: viewing directions parallel to the grooves (vertically striped bars) or perpendicular to the grooves (horizontally striped bars).

the surface, as discussed below. In an attempt to quantify the anisotropy of the drop shape, the ratio of the drop dimensions in two perpendicular directions was calculated. As expected, the ratio was close to 1.0 for drops on square microstructures, whereas a strong deviation was found for grooved surfaces of pristine ETFE (1.3) and of ETFE modified with neutral and weak PEL brushes (PVMP: 2.1; P4VP 1.9). Noticeably, the droplet volume had no influence on the drop shape ratio in the range investigated (2−10 μL). This observation can be attributed to the fact that the drops were large compared to the microstructure dimensions, thus eliminating the drop-size dependences that were reported for drops of submicroliter volume.[10]

Furthermore, images of the droplets in side view were used to evaluate the CAs in different directions. In the case of square microstructures, the CAs were determined in directions along the square edge axis and in the direction of the square diagonal, whereas on grooved substrates, directions perpendicular and parallel to the grooves were considered. The results are given in Figure 3C and compared to the CAs measured on flat substrates with the same surface chemistry.[14] Clearly, the same observations as for the drop shape also apply when discussing contact angles. Surface modification with the ionic QP4VP led to very low contact angles, regardless of the surface topography. The highly hydrophilic polyelectrolyte brush is swellable in water and probably allows water to easily penetrate gaps in the microstructure. Consequently, pinning effects are not observed in this case as the spreading of the water droplet is not hindered. In contrast, pinning leads to CAs exceeding the values found on flat substrates in the case of structured ETFE, P4VP and PVMP surfaces. The increase in CAs compared to flat substrates caused by pinning effects was strongest for the neutral and weak PEL brushes (PVMP and P4VP). The anisotropy of the substrates is furthermore reflected in the differing contact angles observed along different sample directions. For the highly anisotropic drop on the grooved neutral surface (PVMP), the CA perpendicular to the grooves ($CA_{\perp}$) was as much as 37° lower than the CA parallel to the grooves ($CA_{\parallel}$). The effect was also very strong on the weak PEL surfaces. Noticeably, the CAs measured in different directions on substrates with squares differed less, as expected from the less pronounced anisotropy of the microstructure.

The drop shapes shown in panels A and B in Figure 3 result from the restrictions placed on a drop spreading on a structured surface.[8] Upon spreading, the drop will repeatedly encounter the gaps separating the square or line features of the microstructure. The three-phase contact line of the droplet is pinned on the ridges of the structure, as an energy barrier needs to be overcome in order for the liquid to bridge these gaps or grooves. Consequently, the final drop shape is determined by the pinning of the contact line on features of the microstructure. This phenomenon can be illustrated best when viewing the sample from below, i.e. by taking pictures of the footprint of the droplet through the transparent substrate. In Figure 4A, the corresponding images showing the pinning of contact lines of 2 μL sized droplets along rows of squares or along grooves of surfaces modified with weak PEL brushes are given. Clearly, the straight sections of the contact line strictly follow the preferential direction of the microstructures. The behavior of a spreading droplet on a surface with grooves is illustrated by a series of images recorded while increasing the volume of the droplet (Figure 4B). The contact line of the droplet "hops" from groove to groove when the volume is

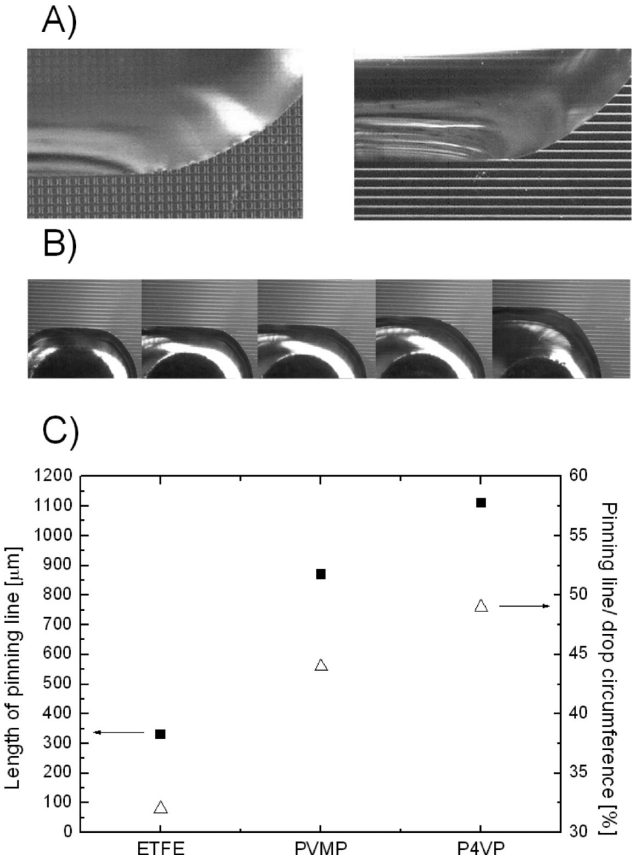

Figure 4. (A) Pinning of contact lines of 2 μL-sized droplets along rows of squares or along grooves of samples modified with basic P4VP brushes. (B) Behavior of a growing droplet on a surface with grooves. Series of snapshots were taken at intervals of 2−4 s, showing hopping of the contact line from groove to groove. (C) Analysis of 2 μL droplet footprints on square microstructures. The length of the pinned, straight contact line was measured and related to the droplet circumference. All images were recorded from below, i.e., drop footprints were characterized.

increased. Moreover, as suggested by the highly variable drop shapes in Figure 3, the surface chemistry has a strong influence on the degree of pinning. Analyzing the footprints of 2 μL droplets on samples with a square microstructure, the length of the straight, pinned sections was established and related to the total droplet circumference. The length of the pinning line increased from ETFE to P4VP, i.e., from hydrophobic to more hydrophilic surfaces (Figure 4C). The share of the pinning line in the total circumference amounted to almost 50% in the case of P4VP. This trend of increasing pinning line length with increasing hydrophilicity of the sample is, however, not continuous, because the footprints of the droplets on very hydrophilic samples modified with ionic QP4VP samples contained no straight sections at all.

Theoretical Considerations. None of the commonly applied models used to describe the influence of (nano)-topography on the water contact angle is able to explain the observed anisotropies in wetting and droplet spreading. First of all, most models do not consider anisotropies in the surface structure. Cassie−Baxter type wetting[17] can be ruled out because the surfaces used are too hydrophilic and the structures too shallow to lead to incomplete wetting of the grooves underneath the droplet, as suggested in this model. Furthermore, the Wenzel model[18] is not applicable, even

though it assumes complete wetting of a rough substrate. However, for hydrophilic surfaces it would predict a decrease in contact angle compared to a flat surface, i.e., the opposite of what was observed. Therefore, the observed effects must be explained chiefly by geometrical constraints. It is a known phenomenon that sharp edges represent energy barriers for the spreading of droplets. Very strong pinning along sharp edges has, for example been found for droplets sitting on posts of different shapes of moderately hydrophilic[19] and of hydrophobic[20] materials. The general understanding is that the contact line is pinned as long as the Gibbs inequality condition is fulfilled.[21] At the discontinuity represented by a sharp edge of 90°, for instance, a maximum increase of 90° in the apparent contact angle with respect to the contact angle at a flat surface would be possible. Making the assumption of sharp edges, the anisotropic shapes of droplets expanding on periodic groove structures or on single rectangular posts[8,22] could be explained.

In contrast to these examples, the pinning in the present study was induced by a shallow structure with smooth, rounded edges. The situation is no longer explicable by a discontinuity at the surface. However, it can be explained by the geometry of the surface. A droplet placed on a groove structure is schematically depicted in Figure 5. Under equilibrium

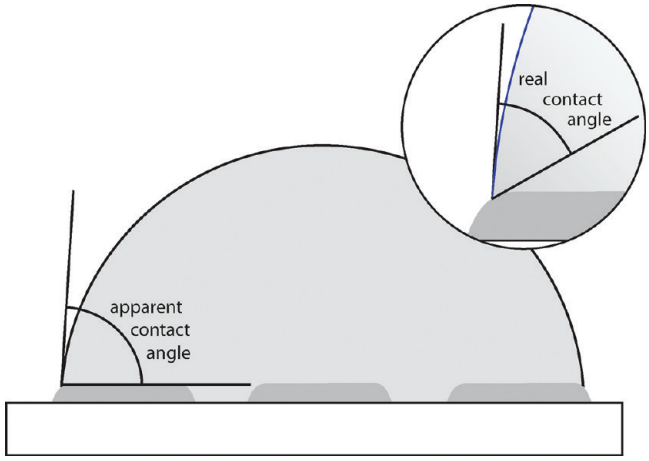

Figure 5. Schematic representation of a droplet placed on a line structure viewed in parallel to the grooves. The close-up demonstrates how shifting of the pinning line into the curved region at the top of the structure leads to a larger apparent contact angle.

conditions, the contact line will shift into the curved region at the edge. This results in an increase in apparent contact angle without any change of real contact angle. The observed drop shapes result from the minimization of the total surface energy and the energetic minimization of the surface-to-volume ratio of the droplet. This ratio is determined by the apparent contact angle and not by the real contact angle.

On the presented surfaces, the spreading of water perpendicular to the grooves is efficiently hindered by surface structure. In contrast, the expansion parallel to the grooves is not hindered and it is determined by the hydrophilicity of the substrate. This explains why the anisotropy of the wetting increases with increasing hydrophilicity. In the case of the ionic QP4VP modification, wetting is predominant and pinning at the rounded edges is no longer observed.

In the case of the square structures, pinning lines are repeatedly interrupted by the perpendicular grooves, through which the wetting can proceed. Therefore, even though pronounced pinning along rows of squares is observed, only very limited increase in apparent contact angle is possible.

Effect of Anisotropic Substrate Topography on the Sliding Behavior of Droplets. The sliding behavior of a droplet on grooved ETFE and ETFE substrates modified with basic Q4VP is illustrated in Figure 6. Although the drop started

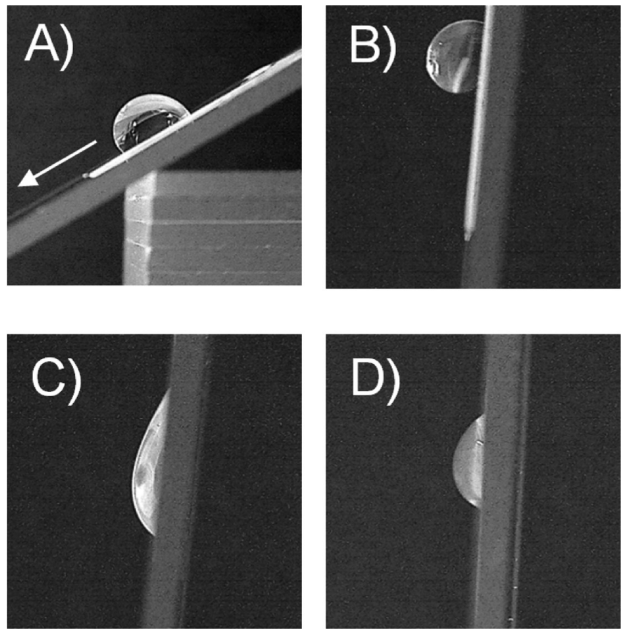

Figure 6. Behavior of 10 μL droplets placed on different surfaces: (A) on ETFE, parallel to the grooves; the sliding angle is 31 ± 5°; (B) on ETFE, perpendicular to the grooves, the droplet does not slide even if the substrate is tilted to a vertical position. On the weak PEL-modified surface (P4VP), no sliding was observed, either (C) parallel, or (D) perpendicular to the grooves.

moving on ETFE along the direction parallel to the grooves at a tilt angle of about 30°, no sliding was observed in the direction perpendicular to the grooves, even if the substrate was tilted to a vertical orientation. This observation illustrates another highly anisotropic surface property which, similar to the rice leaf structure, guides water in one direction and prevents it from sliding off the surface in the other. However, drop movement was completely inhibited on the more hydrophilic P4VP surfaces in both directions. In this case, the footprint of the drop was too large to enable its sliding along the grooves of the microstructure, i.e., along the easy axis of sliding. Therefore, this is yet another example of surface topography and chemistry critically influencing the anisotropic properties of a surface.

Wettability Gradients on Structured Substrates. Inducing drop movement on a surface usually requires the assistance of gravity as illustrated in Figure 6. As outlined in the introduction, spontaneous drop movement can also be provoked by variation of surface roughness or surface energy.[11,12] However, to obtain appreciable effects using these approaches, quite stringent conditions need to be fulfilled. For instance, surface topography must be designed and controlled in the micrometer range or, in the second case, CA variation must be large and the CA hysteresis low.

In the present work, structured substrates with a simple anisotropic topography without spatial variation were endowed with yet another directional surface property, i.e. a chemical gradient, to obtain new wetting properties. To test this concept,

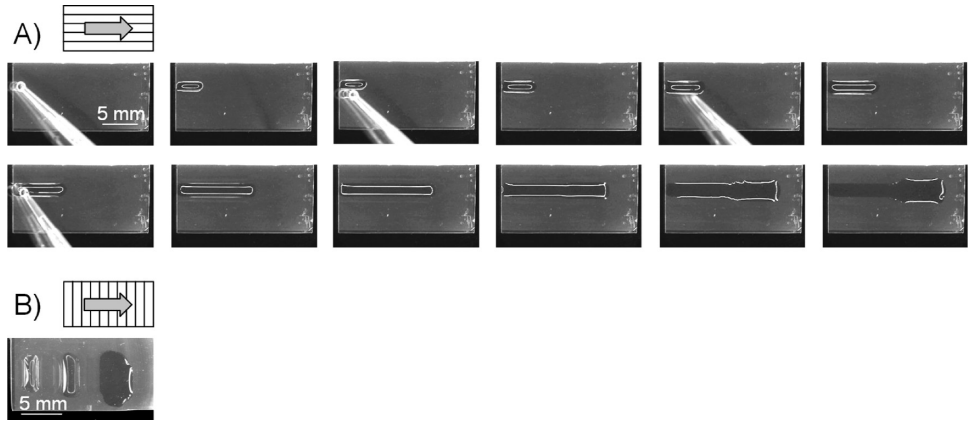

Figure 7. Illustration of the spreading of water droplets on surfaces with periodic grooves and a superimposed polymer brush wettability gradient. The cartoons illustrate the orientation of the grooves and the direction of the gradient (arrow pointing from the high CA to the low CA side. (A) First row: Series of snapshots showing how three droplets (1.5 μL each) were dispensed on the high CA side of the gradient. Second row: dispensing of a fourth droplet results in spreading over the whole length of the gradient and dewetting on the high CA side. (B) Photograph of drop spreading on a surface having the gradient direction oriented perpendicularly to the hot embossed grooves.

a chemical gradient containing variable proportions of *N*-methyl-vinylpyridinium and *N*-methyl-2-pyridone functionalities was prepared. The slow conversion of QP4VP brushes to PVMP brushes in alkaline media was exploited, as described earlier.[15] Briefly, the ionic polyelectrolyte (QP4VP) brush is gradually transformed into the neutral PVMP brush by slow immersion into sodium hydroxide solution. As a result, the CAs as assessed on flat surfaces varied from about 60° at the PVMP-rich end of the gradient to about 10° at the QP4VP-rich end of the gradient. The gradient produced in this manner covered intermediate-to-low CAs, ensuring highly elongated drop shapes at the more hydrophobic end of the gradient. This was promising in terms of obtaining directional wetting properties.

In Figure 7A, the spreading of water droplets placed on a sample with a freshly prepared gradient oriented parallel to the microstructure is shown. The series of snapshots illustrates how the consecutive placement of four water droplets (1.5 μL each) at the high CA side of the gradient first resulted in an elongation of the droplet. When a certain volume was reached, the water spread quickly across the whole length of the gradient. A considerably broader area was wetted at the low CA end of the gradient, while the amount of water in regions with poorer wettability was reduced. Note that this was observed on a horizontally placed sample, i.e., the directed spreading over a distance of over 16 mm was not assisted by tilting of the sample. The spreading direction was from the high to the low contact angle side of the gradient, in line with the observation that a drop on the right (low CA) end of the gradient did not spread toward the higher CA regions. In Figure 7B, the effect of a gradient perpendicular to the microstructure direction is shown. The drops exhibited a highly anisotropic shape with the main axis aligned to the microstructure orientation and a position-dependent width due to the superimposed wettability gradient. Consequently, a variation of drop shapes resulted along the gradient.

The observations detailed above demonstrate the strong mutual enhancement of two surface characteristics, the topographic anisotropy of the substrate and a directional gradient in wettability, and support the strategy of combining different incentives for directed drop spreading. In the case of a parallel alignment of the gradient to the grooves, the two ends of the drop were sufficiently far apart to experience the gradient in wettability because of the elongated drop shape induced by the microstructure. Apparently, the difference in CAs on the two ends of the elongated drop was large enough to create a driving force for spreading in the direction of lower CA. By contrast, creating a gradient perpendicular to the groove-microstructure led to a conflict in directionality, resulting in different drop shapes along the gradient with the main direction being determined by the microstructure orientation.

CONCLUSION

Wetting phenomena such as drop-shape anisotropy, contact-angle anisotropy and contact-line pinning were studied on microstructured surfaces with different surface chemistries. A straightforward and versatile method for producing this type of sample was presented, in which the type and period of the hot embossed microstructure can be selected by using different stamps. Moreover, apart from the P4VP, PVMP, and QP4VP brushes presented here, a variety of other monomers can be grafted from ETFE, enabling tailor-made surface chemistry and wettability of the foil, as shown previously.[14] Structured substrates modified with the ionic QP4VP brushes are also attractive platforms for tailoring the wettability via exchange of the counter-anions to the quaternary ammonium moieties.[23−25]

As shown in this study, both the surface topography and the functionality of the surface had a strong influence on the shape of water droplets, and, consequently, on the CA of the surface. Pinning was induced on ETFE and on surfaces modified with neutral and weak PEL (PVMP and P4VP) brushes by groove structures without sharp edges, leading to anisotropic drop shapes and an increase in CAs with respect to flat surfaces. CAs determined along the preferential directions of a given sample differed significantly (by up to 37°).

To test a new concept for directed drop spreading, we combined two directional surface properties, i.e., anisotropic topography and a gradient in polymer brush composition. With the knowledge that intermediate CA lead to the highest drop shape anisotropy, a wettability gradient spanning a range from intermediate to very hydrophilic CAs was selected and spontaneous drop movement was observed. Noticeably, neither an intricate topography nor a very high difference in CA was required to obtain the desired effect. Moreover, the use of this

concept is not limited to the presented system because, for instance, the preparation of a self-assembled monolayer gradient on a structured silicon substrate is also conceivable to obtain the same effect.

AUTHOR INFORMATION

Corresponding Author
*E-mail: celestino.padeste@psi.ch.

ACKNOWLEDGMENTS

The authors thank Konrad Vogelsang for the preparation of the hot-embossed substrates, Anja Weber for the SEM investigations, and Dr. Doris M. Spori for invaluable discussions on theoretical aspects. The financial support of the Swiss National Science Foundation (SNF) is greatly appreciated.

REFERENCES

(1) Zhu, D. F.; Li, X. A.; Zhang, G.; Zhang, X.; Zhang, X. M.; Wang, T. Q.; Yang, B. *Langmuir* **2010**, *26*, 14276−14283.
(2) Zheng, Y. M.; Gao, X. F.; Jiang, L. *Soft Matter* **2007**, *3*, 178−182.
(3) Liu, M. J.; Zheng, Y. M.; Zhai, J.; Jiang, L. *Acc. Chem. Res.* **2009**, *43*, 368−377.
(4) Feng, L.; Li, S. H.; Li, Y. S.; Li, H. J.; Zhang, L. J.; Zhai, J.; Song, Y. L.; Liu, B. Q.; Jiang, L.; Zhu, D. B. *Adv. Mater.* **2002**, *14*, 1857−1860.
(5) Xia, D. Y.; He, X.; Jiang, Y. B.; Lopez, G. P.; Brueck, S. R. J. *Langmuir* **2010**, *26*, 2700−2706.
(6) Yoshimitsu, Z.; Nakajima, A.; Watanabe, T.; Hashimoto, K. *Langmuir* **2002**, *18*, 5818−5822.
(7) Long, C. J.; Schumacher, J. F.; Brennan, A. B. *Langmuir* **2009**, *25*, 12982−12989.
(8) Chung, J. Y.; Youngblood, J. P.; Stafford, C. M. *Soft Matter* **2007**, *3*, 1163−1169.
(9) Morita, M.; Koga, T.; Otsuka, H.; Takahara, A. *Langmuir* **2005**, *21*, 911−918.
(10) Yang, J.; Rose, F.; Gadegaard, N.; Alexander, M. R. *Langmuir* **2009**, *25*, 2567−2571.
(11) Sun, C.; Zhao, X. W.; Han, Y. H.; Gu, Z. Z. *Thin Solid Films* **2008**, *516*, 4059−4063.
(12) Chaudhury, M. K.; Whitesides, G. M. *Science* **1992**, *256*, 1539−1541.
(13) Zheng, Y. M.; Bai, H.; Huang, Z. B.; Tian, X. L.; Nie, F. Q.; Zhao, Y.; Zhai, J.; Jiang, L. *Nature* **2010**, *463*, 640−643.
(14) Neuhaus, S.; Padeste, C.; Spencer, N. D. *Plasma Process. Polym.* **2011**, *8*, 512−522.
(15) Neuhaus, S.; Padeste, C.; Spencer, N. D. *Langmuir* **2011**, *27*, 6855−6861.
(16) Farquet, P.; Kunze, A.; Padeste, C.; Solak, H. H.; Guersel, S. A.; Scherer, G. G.; Wokaun, A. *Polymer* **2007**, *48*, 4936−4942.
(17) Cassie, A. B. D.; Baxter, S. *Trans. Faraday Soc.* **1944**, *40*, 0546−0550.
(18) Wenzel, R. N. *Ind. Eng. Chem.* **1936**, *28*, 988−994.
(19) Oliver, J. F.; Huh, C.; Mason, S. C. *J. Colloid Interface Sci.* **1977**, *59*, 568−581.
(20) Toth, T.; Ferraro, D.; Chiarello, E.; Perino, M.; Mistura, G.; Bissacco, G.; Semprebon, C. *Langmuir* **2011**, *27*, 4742−4748.
(21) Kusumaatmaja, H.; Vrancken, R. J.; Bastiaansen, C. W. M.; Yeomans, J. M. *Langmuir* **2008**, *24*, 7299−7308.
(22) Semprebon, C.; Mistura, G.; Orlandini, E.; Bissacco, G.; Segato, A.; Yeomans, J. M. *Langmuir* **2009**, *25*, 5619−5625.
(23) Lim, H. S.; Lee, S. G.; Lee, D. H.; Lee, D. Y.; Lee, S.; Cho, K. *Adv. Mater.* **2008**, *20*, 4438−4441.
(24) Azzaroni, O.; Brown, A. A.; Huck, W. T. S. *Adv. Mater.* **2007**, *19*, 151−154.
(25) Wang, L. M.; Peng, B.; Su, Z. H. *Langmuir* **2010**, *26*, 12203−12208.